MECSOL 2022 - Proceedings of the 8th International Symposium on Solid Mechanics
M.L. Bittencourt, J. Labaki, L.C.M. Vieira Jr. and E. Mesquita (Editors), Campinas SP, Brazil, October 17th to 19th, 2022

Sensitivity analysis for the topology optimization of bimorph piezoelectric energy harvesters for voltage maximization

Breno Vincenzo de Almeida[1], Renato Pavanello[1]

[1]Department of Computational Mechanics, School of Mechanical Engineering, University of Campinas. Mendeleyev St, 13880, Campinas, Brazil

The design of a bimorph cantilevered-type piezoelectric energy harvesting device subject to base vibration can be determined via a topology optimization procedure using the BESO method. The device is modeled considering plane strain hypothesis, harmonic base vibration, Rayleigh damping and a simple resistor connecting the electrodes. In such optimization problems, it is common to consider a performance parameter dependent on energy terms, such as the electromechanical coupling coefficient or the ratio between input mechanical work and output electrical energy. Another option is to directly maximize the electrical power dissipated in an equivalent electrical circuit connecting the electrodes, which can present instabilities in the optimization process if no energy terms are considered. In this work, sensitivity analyses are performed for the latter case, seeking to investigate the suitability of conventional sensitivity analysis procedures for this class of problems when applied to discrete optimization problems such as the BESO method.

Keywords: topology optimization, piezoelectric materials, energy harvesting, sensitivity analysis

INTRODUCTION

Piezoelectric energy harvesters (PEH) can be utilized to convert vibrational waste energy into useful electrical energy to power small electromechanical systems for remote sensing and continuous monitoring applications, which has increased considerably since the advent of Industry 4.0. Their use is an environmentally friendlier option in comparison to utilizing batteries, which are considerably pollutant and have to be replaced regularly (Covaci and Gontean, 2020). There are many types of configurations for PEHs, but the most common one is the cantilevered-beam type harvester, which exhibits a larger mechanical quality factor than most of the other types and is easier to manufacture (Shahab et al., 2018; Covaci and Gontean, 2020).

It is therefore of interest to optimize the shape of the PEH in order to maximize its power output. Topology optimization (TO) can be applied to this end. In TO the design of a device is firstly numerically described using a discretization technique, such as the Finite Element Method (FEM), and the discretized units may become design parameters of an optimization problem, seeking to minimize (or maximize) some performance parameter dependent on its material layout. The Solid Isotropic Material with Penalization (SIMP) (Bendsøe and Sigmund, 2004) is the most widely used method in the category of continuous density-based methods and the Bidirectional Evolutionary Structural Optimization (BESO) method is one of the most widely utilized methods in the category of evolutionary TO methods (Huang and Xie, 2010).

In this work, the BESO method is utilized, since it is easier to obtain discrete topologies at every iteration of the optimization process, without having to resort to any projection or filtering techniques. This is useful for the optimized placement of electrodes during the optimization process (de Almeida et al., 2019).

Many articles in the literature perform TO in PEHs by optimizing a performance parameter related to the strain energy of the device, such as the electromechanical coupling coefficient (Zheng et al., 2008; Noh and Yoon, 2012; Vatanabe et al., 2013; de Almeida et al., 2019; Homayouni-Amlashi et al., 2020) in order to stabilize the optimization process. The strain energy is also utilized in the optimization of dynamic systems as multi-objective functions to further stabilize the process, but this can lead to far from optimal designs (Silva et al., 2019).

Instead, in this work, the power dissipated in a resistor connecting the electrodes of the PEH is taken as the performance parameter (Vatanabe et al., 2012; Kiyono et al., 2016). The main goal is to analyze whether the common method of calculating the sensitivities, i.e. the derivative of the objective function with respect to (wrt) the design variables, is suitable for this sort of optimization process, considering that the design variables are discrete, having the BESO method in mind. The analytical sensitivities are firstly developed and calculated and are then validated by comparing them sensitivities obtained via finite differences, specifically through a central difference scheme. Finally, since the BESO method considers discrete design variables, the analytical sensitivities are compared to “naive sensitivities”, in which

the sensitivity of each element is calculated as the change in the objective function for a discrete design variable change (Cunha et al., 2021).

Figure 1 shows a two-dimensional (2D) slice of a middle longitudinal section of a device. Specifically, it shows a bimorph cantilevered PEH with series connection, since it has two piezoelectric layers (shown in blue) with inverse polarization directions (as indicated by the green arrows) and an intermediate metallic substrate. The upper and lower yellow regions are the electrodes. They are connected to each other with a resistor R. No external forces are applied to the harvesting devices. The device is clamped on the left-hand side, where harmonic base vibration occurs. The intermediate metallic substrate is grounded.

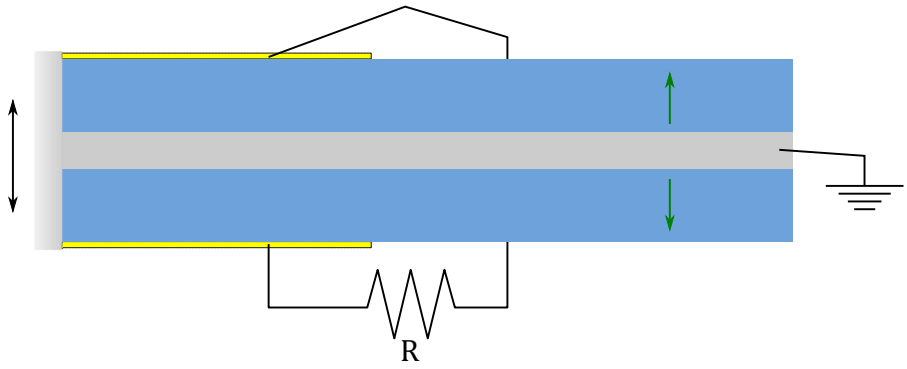

Figure 1 – Plane strain piezoelectric energy harvester model

Linear hypotheses are considered for the analysis, i.e. linear piezoelectric constitutive equations, small displacements and small strains. The piezoelectric layers are perfectly glued to the metallic substrate and the electrodes adhere perfectly to the piezoelectric layers, with negligible stiffness and inertia.

NUMERICAL ANALYSIS

The FEM is applied to discretize the bimorph piezoelectric energy harvester considering 2D plane strain hypothesis and harmonic base vibration of frequency ω. The resulting linear system of equations shown in Eq. (1) is solved to find the amplitudes of the nodal displacements u and electric potentials ϕ.

$$\begin{bmatrix} \mathbf{K}_{uu} + j\omega\mathbf{C} - \omega^2\mathbf{M} & \mathbf{K}_{\phi u}^T & 0 \\ \mathbf{K}_{\phi u} & j\omega\mathbf{C}_R - \mathbf{K}_{\phi\phi} & \Lambda_\phi^T \\ 0 & \Lambda_\phi & 0 \end{bmatrix} \begin{Bmatrix} u \\ \phi \\ l \end{Bmatrix} = \begin{Bmatrix} 0 \\ 0 \\ 0 \end{Bmatrix} \tag{1}$$

where $\mathbf{K}_{uu}$, $\mathbf{K}_{\phi u}$ and $\mathbf{K}_{\phi\phi}$ are the elastic stiffness, piezoelectric and dielectric global matrices, respectively. $\mathbf{M}$ is the global mass matrix. $\mathbf{C} = \alpha\mathbf{M} + \beta\mathbf{K}_{uu}$ is the damping matrix, considering Rayleigh damping, with $\alpha = 0$ and $\beta = 10^{-6}$. j is the imaginary unit $\sqrt{-1}$, and ω is the frequency of the base vibration. Since the electric potentials of the nodes that belong to the electrodes are equal to each other but unknown *a priori*, Lagrange multipliers are utilized to impose these equality constraints. The sparse matrices Λ_ϕ are used to this end. The vector l contains the Lagrange multipliers. Finally, the damping matrix $\mathbf{C}_R$ models the dissipation due to the electrical current passing through the resistor R, which connects the upper and lower electrodes. It is calculated as shown in Eq. (2).

$$\mathbf{C}_R = \frac{1}{\omega^2 R} \begin{bmatrix} 1 & -1 \\ -1 & 1 \end{bmatrix} \tag{2}$$

Due to the mechanical Rayleigh damping and to the dissipative effects of the resistor, the matrix shown in Eq. (1) is complex. Also, it is symmetric with an indefinite real part. Therefore, u and ϕ are also complex. The linear system can be succinctly written as $\mathbf{K}_g U = 0$.

Equation (1) has 0's in the right-hand side, since no external forces are applied to the system. By applying harmonic base vibration of the type $u = u_{pd} e^{j\omega t}$, the rows of the prescribed degrees of freedom can be removed and the corresponding columns of the global stiffness matrix $\mathbf{K}_g$ can be multiplied by the prescribed nodal displacements and passed to the right-hand side through a subtraction operation. Therefore, the reduced system of equations is obtained:

$$\tilde{\mathbf{K}}_g \tilde{U} = \tilde{f}_{pd} \tag{3}$$

where the tilde represents the reduced system and the subscript *pd* indicates "prescribed displacements".

OPTIMIZATION FORMULATION

The power output of the modeled PEH can be calculated as the energy dissipated in the resistor. For a constant resistance R this energy W may be calculated as shown in Eq. (4), where $\Delta\phi$ is the electric potential difference between the electrodes and the overline represents the complex conjugate of a complex scalar (Vatanabe et al., 2012). Note that, although this parameter is a measure of energy, it is not directly dependent on the strain energy of the device.

$$W = \frac{\overline{\Delta\phi}\Delta\phi}{2R} \tag{4}$$

The goal is to maximize this parameter, or equivalently to minimize its negative value, so the following TO problem can then be defined:

$$\begin{aligned} \min_{x} \quad & \eta = -\frac{\overline{\Delta\phi}\Delta\phi}{2R} \\ \text{s.t.} \quad & \tilde{\mathbf{K}}_g \tilde{U} = \tilde{f} \\ & \sum_i V_i = V_t \\ & x_i \in \{0,1\} \end{aligned} \tag{5}$$

where x is a vector containing 1's and 0's for each element if they are solid or void, respectively. V_i is the volume of the i-th element and V_t is the target volume.

The sensitivities are then obtained by differentiating η by x_i, yielding:

$$\frac{\partial\eta}{\partial x_i} = -\frac{1}{2R}\left(\frac{\partial\overline{\Delta\phi}}{\partial x_i}\Delta\phi + \overline{\Delta\phi}\frac{\partial\Delta\phi}{\partial x_i}\right) = -\frac{1}{R}\Re\left(\overline{\Delta\phi}\frac{\partial\Delta\phi}{\partial x_i}\right) \tag{6}$$

where $\Re$ denotes the real part.

The scalar complex value $\Delta\phi$ can be written as $L^T U$, where the vector L is a vector of zeros with 1 and -1 in the degree of freedom corresponding to one node of the upper electrode and one node of the bottom electrode, respectively. Thus, the sensitivities are equivalent to:

$$\frac{\partial\eta}{\partial x_i} = -\frac{1}{R}\Re\left(\overline{\Delta\phi}L^T\frac{\partial U}{\partial x_i}\right) \tag{7}$$

Since the prescribed displacements are constant throughout the optimization process, they are also constant wrt x_i. Thus, their derivative wrt to x_i is 0. Therefore:

$$\frac{\partial U}{\partial x_i} = \begin{Bmatrix} \frac{\partial\tilde{U}}{\partial x_i} \\ 0 \end{Bmatrix} \tag{8}$$

And $\frac{\partial\tilde{U}}{\partial x_i}$ can be found by differentiating the equilibrium equation Eq. (3) by x_i, obtaining:

$$\frac{\partial\tilde{U}}{\partial x_i} = \tilde{\mathbf{K}}_g^{-1}\left(\frac{\partial\tilde{f}_{pd}}{\partial x_i} - \frac{\partial\tilde{\mathbf{K}}_g}{\partial x_i}\tilde{U}\right) \tag{9}$$

Substitution of Eq. (9) into Eq. (7) yields:

$$\frac{\partial\eta}{\partial x_i} = -\frac{1}{R}\Re\left(\overline{\Delta\phi}\tilde{L}^T\mathbf{K}_g^{-1}\left(\frac{\partial\tilde{f}_{pd}}{\partial x_i} - \frac{\partial\tilde{\mathbf{K}}_g}{\partial x_i}\tilde{U}\right)\right) \tag{10}$$

Since $\tilde{\mathbf{K}}_g$ is symmetric, the following adjoint problem can be solved:

$$\tilde{\mathbf{K}}_g\begin{Bmatrix}\tilde{\lambda}\\ \tilde{\mu}\\ \tilde{\chi}\end{Bmatrix} = \tilde{\mathbf{K}}_g\tilde{\Gamma} = \overline{\Delta\phi}\tilde{L} \tag{11}$$

And the sensitivities are then:

$$\frac{\partial \eta}{\partial x_i} = -\frac{1}{R}\Re\left(\tilde{\Gamma}^T\left(\frac{\partial \tilde{f}_{pd}}{\partial x_i} - \frac{\partial \tilde{\mathbf{K}}_g}{\partial x_i}\tilde{U}\right)\right) \tag{12}$$

And it can be easily verified by comparing the following results with a finite differentiation scheme that the calculation of the sensitivities can be further simplified by considering the unconstrained matrices and vectors:

$$\frac{\partial \eta}{\partial x_i} = \frac{1}{R}\Re\left(\Gamma^T\frac{\partial \mathbf{K}_g}{\partial x_i}U\right) \tag{13}$$

where the unconstrained vector Γ contains zeros in the degrees of freedom corresponding to that of the prescribed displacements. The complete sensitivities are then:

$$\alpha_i = \frac{\partial \eta}{\partial x_i} = \frac{1}{R}\left(\lambda^T\frac{\partial \mathbf{K}_{uu}}{\partial x_i}u + j\omega\lambda^T\frac{\partial \mathbf{C}}{\partial x_i}u - \omega^2\lambda^T\frac{\partial \mathbf{M}}{\partial x_i}u + \lambda^T\frac{\partial \mathbf{K}_{\phi u}^T}{\partial x_i}\phi + \mu^T\frac{\partial \mathbf{K}_{\phi u}}{\partial x_i}u - \mu^T\frac{\partial \mathbf{K}_{\phi\phi}}{\partial x_i}\phi\right) \tag{14}$$

where α_i is a simplified notation for $\frac{\partial \eta}{\partial x_i}$.

Finally, the relationship between the stiffness matrices and the design variables x_i is determined by using the following material interpolation law:

$$\begin{aligned}
\mathbf{K}_{uu}(x_i) &= \left(x_i^{p_0} + (1-x_i^{p_0})x_{min}\right)\mathbf{K}_{uu}^0 \\
\mathbf{K}_{\phi u}(x_i) &= x_i^{p_1}\mathbf{K}_{\phi u}^0 \\
\mathbf{K}_{\phi\phi}(x_i) &= x_i^{p_2}\mathbf{K}_{\phi\phi}^0 + \left(1-x_i^{p_2}\right)\mathbf{K}_{\phi\phi}^{air} \\
\mathbf{M}(x_i) &= \left(x_i^{p_m} + (1-x_i^{p_m})x_{min}\right)\mathbf{M}^0
\end{aligned} \tag{15}$$

where the 0 superscript is the calculated element matrix using FEM, p_0, p_1, p_2 and p_m are the elastic, piezoelectric, dielectric and mass material penalization exponents, respectively. Void elements have the permittivity of air and the ratio between their stiffness and mass matrix values is the same as the ratio for solid elements, thus avoiding local artificial modes of vibration (Huang and Xie, 2010). x_{min} is a small number (e.g. 10^{-4}) that guarantees that the global matrix does not become singular.

ADDITIONAL SENSITIVITIES

In addition to the "analytical sensitivities" derived in the previous section and shown in Eq. (14), this work also considers a finite difference scheme for numerically calculating the sensitivities of each element. It is referred to as "numerical sensitivities" and a central difference formulation was applied, as shown in Eq. (16).

$$\alpha_{numerical}^i = \frac{\eta(x_i+h) - \eta(x_i-h)}{2h} \tag{16}$$

where h is a small number, close to zero.

Finally, an additional method of evaluating whether solid elements should become void or void elements should become solid, is calculating the "naive sensitivities", as defined in (Cunha et al., 2021). These sensitivities are calculated for each element by measuring the difference between the objective function evaluated for when the element is solid and the objective function evaluated for when the element is void. In mathematical terms, the naive sensitivities can be calculated as shown in Eq. (17).

$$\alpha_{naive}^i = \eta(x_i = 1) - \eta(x_i = 0) \tag{17}$$

With the sensitivities defined as shown, positive values indicate that if the element becomes solid, the objective function increases, and negative values indicate that if the element becomes solid, the objective function decreases. Since the goal is to minimize the objective function η, then ideally solid elements should have negative sensitivities and void elements should have positive sensitivities. This interpretation of the sensitivities is exact when observing the naive sensitivities, but is only an approximation when observing the analytical ones, due to the discrete nature of the design variables.

RESULTS

Three possible sensitivity calculations were performed for three different topologies. The sensitivities were obtained considering a 100x25 mm^2 domain discretized by a 100x25 QUAD4 element mesh. Since the electrode positioning

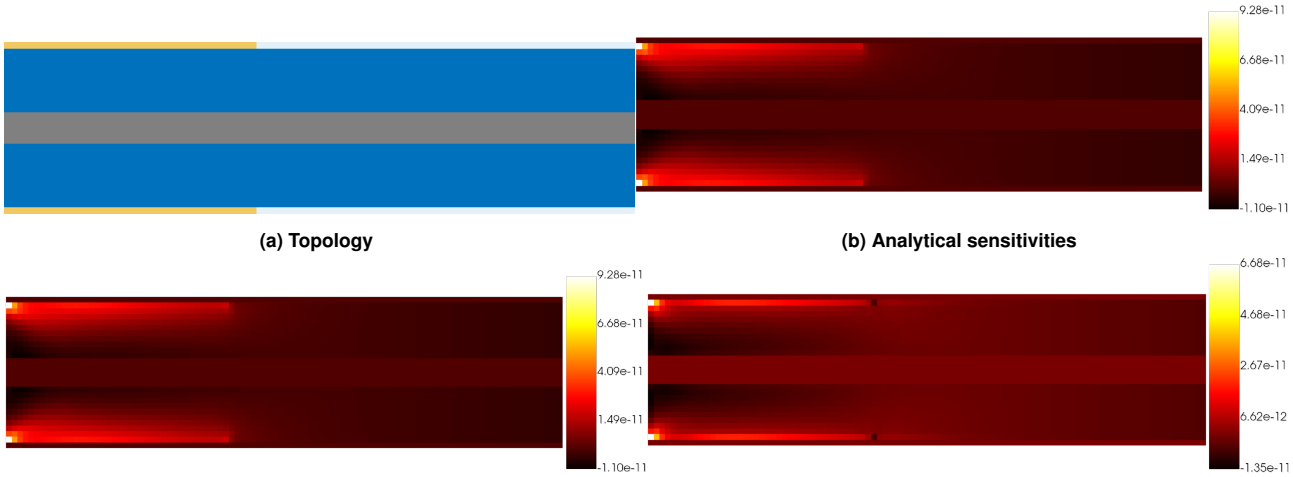

Figure 2 – Full design domain

algorithm of (de Almeida et al., 2019) is used, two additional layers of elements (one above and one below) are added as void non-design domains, so that a clear solid-void piezoelectric surface may exist when the design domain is full. Thus, the whole domain has a $100 \times 27 = 2700$ element mesh.

Additionally, the intermediate metallic substrate of 5 mm in height is also a non-design domain. This coarse mesh was chosen for this analysis, since two Finite Element (FE) analyses must be performed per element to obtain the numerical sensitivities and one FE analysis per element must be performed for the naive sensitivities. A harmonic moving base vibration of 1 nm amplitude vibrating at 500 Hz was considered as input, with a resistor $R = 10k\Omega$. A 40 mm long electrode is applied to the upper and lower surfaces.

The intermediate metallic substrate is steel, with elastic constant $E = 200\ GPa$, Poisson's ratio of $\nu = 0.29$ and specific mass of $\rho = 7860\ kg/m^3$. The piezoelectric material was PZT-4 with elastic constants $c_{11}^E = 168\ GPa$, $c_{13}^E = c_{23}^E = 74.28\ GPa$, $c_{33}^E = 115.4\ GPa$ and $c_{xzxz}^E = c_{44}^E = 25.64\ GPa$; piezoelectric coupling constants $e_{51} = 12.1\ C/m^2$, $e_{31} = -5.2\ C/m^2$ and $e_{33} = 15.1\ C/m^2$; and relative permittivities $\varepsilon_{11}^S = 762.6$ and $\varepsilon_{33}^S = 663.225$, where the E and S superscripts indicate that the properties are taken under constant electric field and strain, respectively. The specific mass of PZT-4 was $\rho = 7500\ kg/m^3$.

In all cases a minimum value for void elements $x_{min} = 10^{-4}$ was utilized and the parameter h for calculating the finite difference scheme was 10^{-3}.

Full design domain

In this section the sensitivities are calculated for the topology shown in Fig. 2a, with the whole possible piezoelectric domain consisting of solid elements. The different sensitivities can be found in Fig. 2. The electric potential difference between the electrodes is $\Delta\phi = 3.620 + j5.114$ mV.

The numerical and analytical sensitivities are qualitatively identical, as can be seen by comparing Fig. 2b to Fig. 2c. The maximum relative difference between the analytical and numerical sensitivities was $8.2 \cdot 10^{-4}$.

Additionally, it can be seen that most of the maximum and minimum sensitivity values of the analytical sensitivities shown in Fig. 2b match with those of the naive sensitivities shown in Fig. 2d. This is a favorable indication of the suitability of using first order derivatives to estimate the sensitivities of finite variations of piezoelectric elements for the maximization of the power dissipated in the resistor.

Strain-penalized design

In this section the sensitivities are calculated for the topology shown in Fig. 2a. This type of topology can be obtained by optimizing the harvesting device for the maximization of the electromechanical coupling coefficient and penalizing the strain energy term (de Almeida et al., 2019). The different sensitivities can be found in Fig. 3. The amplitude of the electric potential difference between the electrodes is $\Delta\phi = 1.741 + j2.299$ mV, which is lower than before.

As in the previous case, the analytical and numerical sensitivities are qualitatively identical, according to Figs. 3b and 3c. The maximum relative difference between them was $3.18 \cdot 10^{-2}$, but between the solid elements the maximum relative difference was only $6.52 \cdot 10^{-4}$.

And similarly to the previous section, the naive sensitivities for this topology has many maximum and minimum sensitivity values matching with those of the analytical sensitivities, as can be seen in Figs. 3d and 3b.

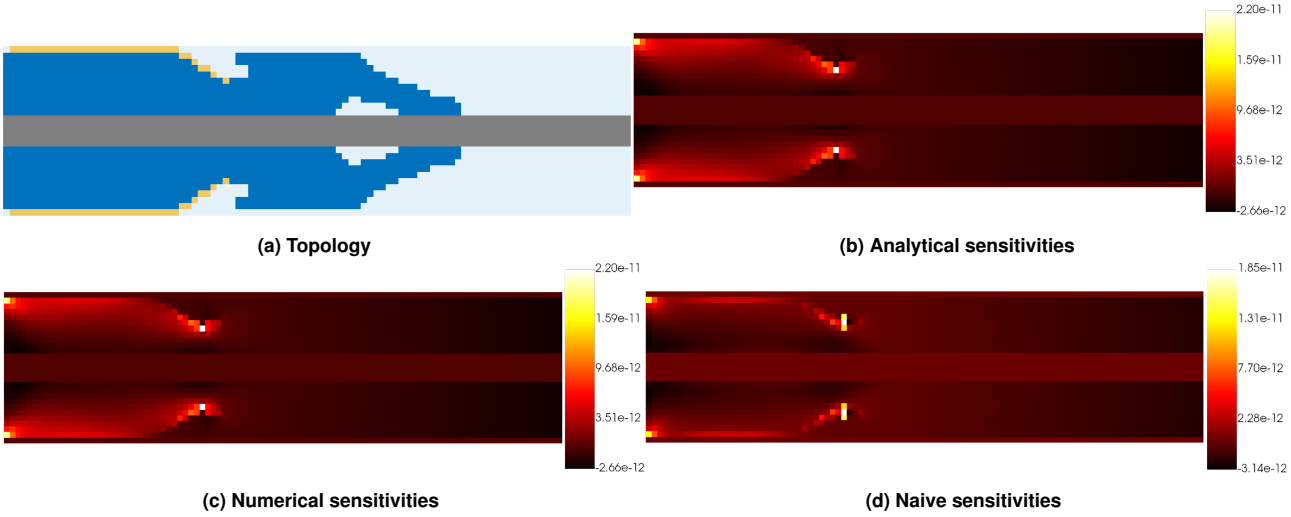

(a) Topology **(b) Analytical sensitivities**

(c) Numerical sensitivities **(d) Naive sensitivities**

Figure 3 – Strain-penalized design

Tip-mass design

In this section the sensitivities are calculated for the topology shown in Fig. 4a. This design has a larger mass concentrated at the free-end of the device, thus having a smaller first natural frequency. The voltage difference between the electrodes for this topology is $\Delta\phi = -6.829 - j168.861$ mV, which is significantly larger in absolute value than the previous two, although most of the value increase occurs in its imaginary part, which is not ideal.

Again, the analytical and numerical sensitivities are qualitatively identical, Again, the analytical and numerical sensitivities are qualitatively identical, as can be seen when comparing Fig. 4b and Fig. 4c. But the maximum relative difference is now $7.66 \cdot 10^{-1}$ when considering all elements and $4.04 \cdot 10^{-3}$ when considering only the solid elements. These larger values can be attributed to floating point errors which occur when operating on values with large magnitude decreases. Another possibility to improve this difference would be to apply numerical preconditioning of the global matrix from Eq. (1) in order to account for the worsening of the condition number due to the existence of void degrees of freedom.

Finally, as with the previous cases, there is a good qualitative match between the distribution of high and low values of the analytical and naive sensitivities, as can be seen from Figs. 4b and 4d.

CONCLUSION

The formulation for the topology optimization of a bimorph cantilevered-type piezoelectric energy harvesting device modelled considering plane strain hypothesis was presented. The model considers harmonic moving base as the input, a resistor connecting the electrodes and Rayleigh damping.

The dynamic system of equations obtained after the application of the FEM was then shown, as well as a formulation for the optimal topology of the device, seeking to maximize the power dissipated in the resistor connecting the electrodes. The analytical sensitivities for the considered optimization parameter were developed and calculated for three different topologies.

Additionally, the analytical sensitivities were compared to numerical sensitivities, obtained by applying a finite difference scheme, and to naive sensitivities, which exactly evaluates the variation of the objective function for discrete variations of the elements in the topology.

The results indicate that the analytical sensitivities developed and shown in Eq. (14) are validated, due to them matching with the numerical sensitivities, and that they seem to be enough to lead to an optimal design, as indicated by their

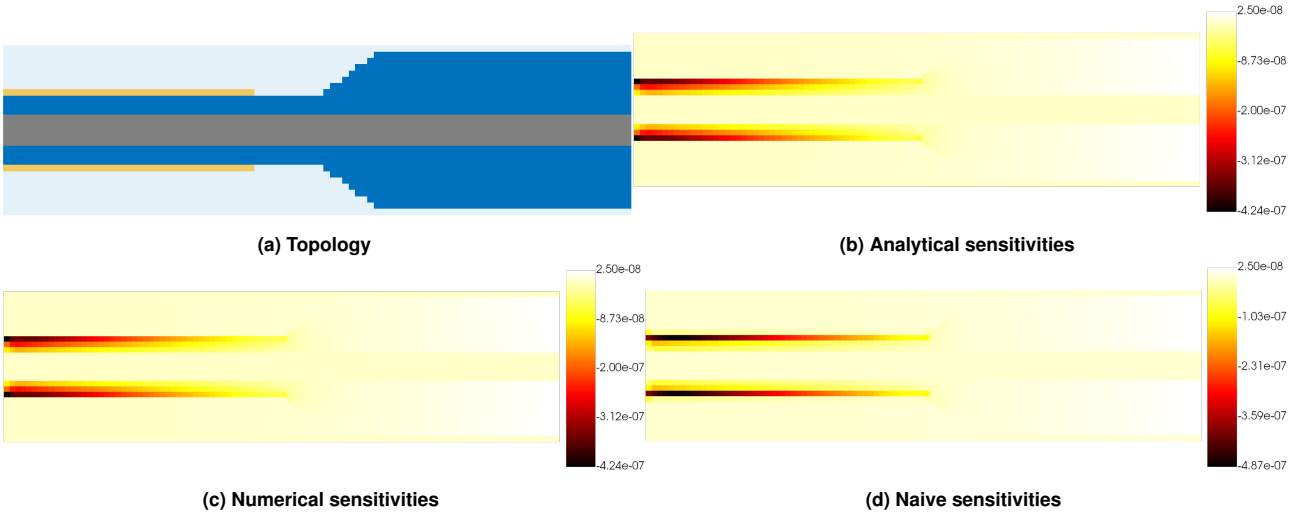

Figure 4 – Tip-mass design

similarity with the naive sensitivities.

Future steps would be to apply the presented methodology to the optimization of the proposed model in 2D and possibly extend it to three dimensions. Additionally, the device can be optimized for different input vibrations or segmented electrodes.

ACKNOWLEDGMENTS

The authors are grateful to FAPESP (São Paulo Research Foundation, grant numbers 2013/08293-7 and 2020/07391-9) for their financial support of this work.

REFERENCES

de Almeida, B.V., Cunha, D.C. and Pavanello, R., 2019, "Topology optimization of bimorph piezoelectric energy harvesters considering variable electrode location", Smart Materials and Structures, Vol. 28, No. 8, p. 085030.

Bendsøe, M.P. and Sigmund, O., 2004, Topology Optimization, Springer Berlin Heidelberg, second edn.

Covaci, C. and Gontean, A., 2020, "Piezoelectric Energy Harvesting Solutions: A Review", Sensors, Vol. 20, No. 12, p. 3512.

Cunha, D.C., de Almeida, B.V., Lopes, H.N. and Pavanello, R., 2021, "Finite variation sensitivity analysis for discrete topology optimization of continuum structures", Structural and Multidisciplinary Optimization, Vol. 64, No. 6, pp. 3877–3909.

Homayouni-Amlashi, A., Mohand-Ousaid, A. and Rakotondrabe, M., 2020, "Topology optimization of 2DOF piezoelectric plate energy harvester under external in-plane force", Journal of Micro-Bio Robotics, Vol. 16, No. 1, pp. 65–77.

Huang, X. and Xie, Y.M., 2010, Evolutionary topology optimization of continuum structures: methods and applications, Wiley, Chichester, West Sussex.

Kiyono, C.Y., Silva, E.C.N. and Reddy, J.N., 2016, "Optimal design of laminated piezocomposite energy harvesting devices considering stress constraints", International Journal for Numerical Methods in Engineering, Vol. 105, No. 12, pp. 883–914.

Noh, J.Y. and Yoon, G.H., 2012, "Topology optimization of piezoelectric energy harvesting devices considering static and harmonic dynamic loads", Advances in Engineering Software, Vol. 53, pp. 45–60.

Shahab, S., Zhao, S. and Erturk, A., 2018, "Soft and Hard Piezoelectric Ceramics and Single Crystals for Random Vibration Energy Harvesting", Energy Technology, Vol. 6, No. 5, pp. 935–942.

Silva, O.M., Neves, M.M. and Lenzi, A., 2019, "A critical analysis of using the dynamic compliance as objective function in topology optimization of one-material structures considering steady-state forced vibration problems", Journal of Sound and Vibration, Vol. 444, pp. 1–20.

Vatanabe, S., Paulino, G. and Silva, E., 2012, "Influence of pattern gradation on the design of piezocomposite energy

harvesting devices using topology optimization", Composites Part B: Engineering, Vol. 43, No. 6, pp. 2646–2654.
Vatanabe, S.L., Paulino, G.H. and Silva, E.C.N., 2013, "Design of functionally graded piezocomposites using topology optimization and homogenization – Toward effective energy harvesting materials", Computer Methods in Applied Mechanics and Engineering, Vol. 266, pp. 205–218.
Zheng, B., Chang, C.J. and Gea, H.C., 2008, "Topology optimization of energy harvesting devices using piezoelectric materials", Structural and Multidisciplinary Optimization, Vol. 38, No. 1, pp. 17–23.

RESPONSIBILITY NOTICE

The authors are the only parties responsible for the printed material included in this paper.